Immobilization of DNA-Au nanoparticles on aminosilane-functionalized aluminum nitride epitaxial films for surface acoustic wave sensing

Chi-Shun Chiu,[1] Hong-Mao Lee,[2] Cheng-Tai Kuo,[2] and Shangjr Gwo[1,2,a)]

[1]*Institute of Nanoengineering and Microsystems, National Tsing-Hua University, Hsinchu 30013, Taiwan*
[2]*Department of Physics, National Tsing-Hua University, Hsinchu 30013, Taiwan*

A generic method for immobilization of gold nanoparticle bioconjugates onto aluminum nitride (AlN) surfaces using aminosilane molecules as cross-linkers is demonstrated for surface acoustic wave (SAW) sensor applications. Electrostatic interaction between positively charged surface amine groups and negatively charged DNA-Au nanoparticle conjugates allows the self-assembly of a probe nanoparticle monolayer onto functionalized AlN surfaces under physiological conditions. Both 10 and 20 nm Au nanoparticles bound with thiolated oligonucleotides were employed in the detection scheme. We show that Au nanoparticles can play multiple roles in SAW sensing for probe immobilization, signal amplification, and labeling. © *2008 American Institute of Physics.*
[DOI: 10.1063/1.3003875]

Surface biochemical functionalization of III-nitride semiconductors (AlN, GaN, and InN) has recently attracted much interest due to their chemical stability, biocompatibility, and multiple device possibilities for biochemical detection.[1,2] For molecular recognition in sensor applications, immobilization of specific molecules on device surface is the first necessary step. Organosilane self-assembled monolayers (SAMs) have been successfully developed as cross-linkers to immobilize, capture, or probe molecules on III-nitride surfaces.[3–5] Moreover, III-nitride electronic devices such as field effect transistors and high electron mobility transistors have been demonstrated for biosensor applications.[6–9] In comparison to transistor-type devices, surface acoustic wave (SAW) sensors offer an alternative approach to perform electrical detection with ultrahigh sensitivity and wide dynamic range.[10] Especially for AlN, due to its large electromechanical coupling coefficient, and SAW propagation velocity, AlN-based SAW devices are very promising for high-frequency, high-sensitivity applications.[11–13] However, to date, only limited studies have been reported for AlN-SAW sensors.[12,13] Here, we report on Au-nanoparticle-enhanced AlN-SAW biochemical sensing utilizing the unique properties of colloidal Au nanoparticles such as high specific weight (mass amplification), availability of a wide range of biofunctionalization schemes, and size uniformity, which are advantageous for quantitative, ultrahigh-sensitivity SAW biodetection.[10]

AlN epitaxial films with a thickness of ~ 1 μm were grown on 3 in. Si(111) substrates by plasma-assisted molecular beam epitaxy (PA-MBE).[14] The Si(111) substrates used here have a low resistivity ranging between 1 and 10 Ω cm. The crystal structure and orientation of PA-MBE-grown AlN epitaxial films were characterized by x-ray diffraction (XRD) and field emission scanning electron microscopy (FE-SEM). A typical ω-2θ diffraction pattern of the AlN films grown on Si(111) substrates is shown in Fig. 1. The XRD results indicate a single crystalline epitaxial structure. The XRD peak at approximately $2\theta=36.08°$ corresponds to the (0002) reflec-

tion of wurtzite AlN, indicating a good alignment of the c-axis with the Si(111) surface normal. The degree of the film orientation along the c-axis was further examined by the (0002) rocking curve (ω scan). The full width at half maximum was determined to be $\sim 0.27°$, significantly smaller than the values reported in the literature.[12,13]

Surface functionalization of AlN films was performed by 3-aminopropyltrimethoxysilane (APTMS) using a protocol described earlier.[4,10] The existence of APTMS SAMs on AlN films was confirmed by x-ray photoelectron spectroscopy (XPS). The XPS spectra were measured with the incoming photon energy of 580 eV at the 09A1 beamline of National Synchrotron Radiation Research Center (NSRRC) in Hsinchu, Taiwan. The binding energy of core level signal was calibrated by the absorbed hydrocarbon C 1s peak. In Fig. 2(a), the XPS peak at 397.1 eV is assigned to the N 1s core-level emission of AlN substrate for both plasma-treated and APTMS-functionalized AlN surfaces. After surface functionalization by APTMS, AlN epitaxial films show additional
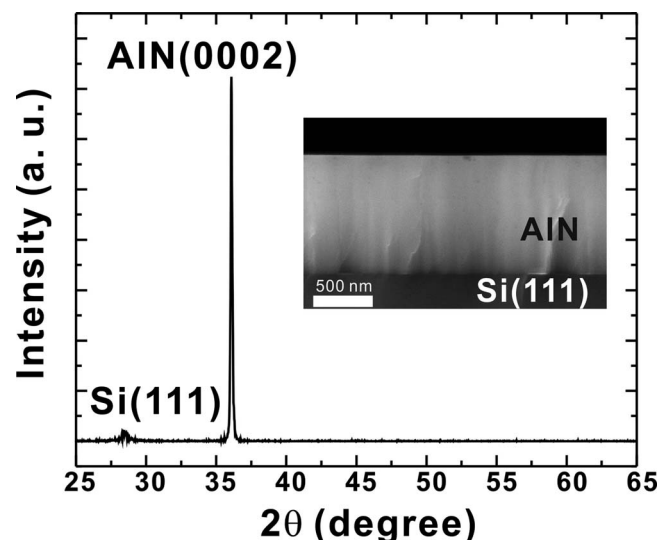

FIG. 1. XRD pattern of the PA-MBE-grown AlN(000$\bar{1}$)/Si(111) structure. The inset shows a cross-sectional FE-SEM micrograph.

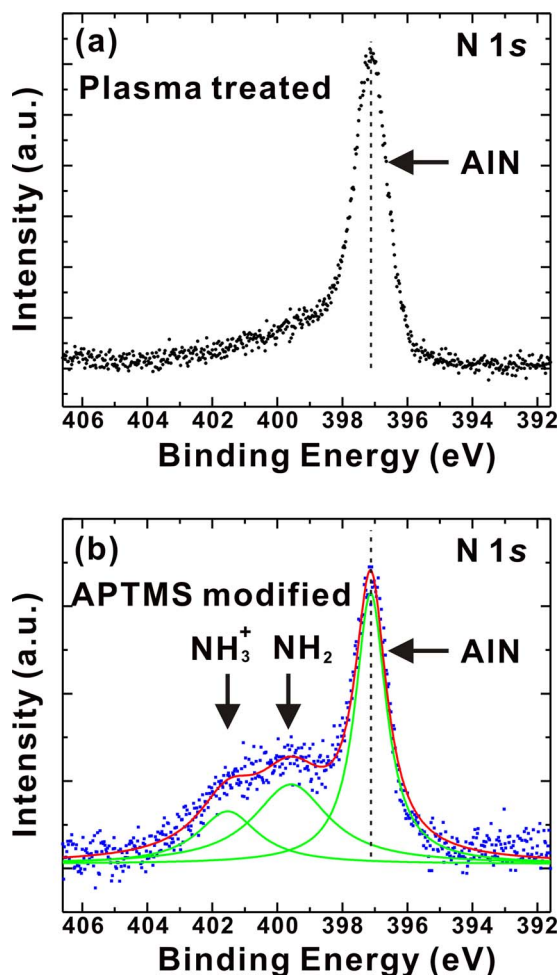a)Author to whom correspondence should be addressed. Electronic mail: gwo@phys.nthu.edu.tw.

FIG. 2. (Color online) Synchrotron XPS spectra of N 1*s* core-level emissions for (a) plasma-treated AlN surface and (b) APTMS-functionalized AlN surface.
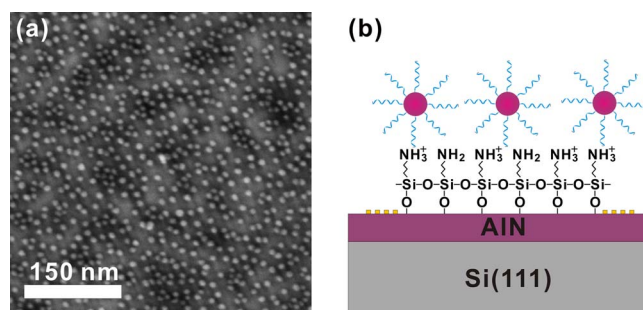

FIG. 3. (Color online) Immobilization (2 h) of probe DNA-Au nanoparticle conjugates on the APTMS-functionalized AlN surface. (a) Surface micrograph obtained by FE-SEM after probe DNA-Au nanoparticle conjugates adsorption. (b) Schematic representation of probe DNA-Au nanoparticle conjugates bound to the APTMS-functionalized AlN surface by electrostatic interaction.

N 1*s* characteristics originating from amine terminal groups. In Fig. 2(b), the XPS spectrum of an APTMS-functionalized AlN surface is shown to exhibit two N 1*s* peaks centered at 401.5 and 399.6 eV, indicating the presence of two types of amine terminal groups on the sample surface: the peak at 399.6 eV is assigned to the uncharged amine groups and that at 401.5 eV is related to the positively charged (protonated) ones (NH_3^+).[4]

In this study, Au nanoparticles were used for DNA probe immobilization, signal amplification (mass-loading enhancement), and labeling in DNA hybridization assay. Citrate-stabilized Au nanoparticles with mean diameters of 10 and 20 nm were purchased from Sigma, and the particle concentrations are ~8 nm and ~1 nM, respectively. The thiolated probe DNA corresponding to the structurally important L2 zinc binding domain of the TP53 gene is a 28-base oligonucleotide with the following sequence:

5′-HS-$(CH_2)_6$

-CATGGTGGGGGCAGTGCCTCACAACCTC-3′.

Also, the target DNA corresponds to the complementary sequence. The molecular weight of oligonucleotide is 8786.79. All water used has a resistivity above 18 MΩ cm. Au nanoparticles were modified with thiolated oligonucleotides according to the salt aging protocol described by Mirkin *et al.*[15] The DNA-Au nanoparticle conjugates were repeatedly

washed and then redispersed in 0.3*M* NaCl, 10 mM phosphate buffer solution (PBS, *p*H 7.5). We estimate that 20% of Au nanoparticles were consumed during this preparation step. In this work, 10 nm Au nanoparticles were modified with probe oligonucleotides and 20 nm Au nanoparticles were modified with target oligonucleotides. In a control experiment, 20 nm Au nanoparticles were modified with probe oligonucleotides for comparison to noncomplementary adsorption.

To understand the process of surface adsorption, the nanoparticle-covered AlN surface was observed by FE-SEM [Fig. 3(a)]. For this purpose, probe DNA-Au nanoparticle conjugates were adsorbed in solution (12.8 nM) onto the APTMS-functionalized AlN surface by electrostatic adsorption between the positively charged APTMS-AlN surface and the negatively charged DNA-Au nanoparticle conjugates [Fig. 3(b)]. The surface density of probe DNA-Au nanoparticle conjugates was found to saturate at ~2730 ± 80 μm^{-2} after a contact time of 1–2 h. This adsorption behavior can be understood by surface charge neutralization due to the adsorbed charged nanoparticles.[10] It should be noted that the required time to reach saturation and the terminal nanoparticle coverage strongly depend on the solution conditions (ionic strength, particle concentration, particle charge state, etc.).

The Rayleigh SAW sensors were fabricated on AlN/Si(111) substrates. The interdigital transducers (IDTs) prepared by 150 nm Al metallization using standard photolithographic process consisted of 50 finger pairs with an acoustic aperture of 1.7 mm, a center to center separation of 5.1 mm, and a periodicity of 34 μm, which corresponds to the SAW wavelength (λ). The measured resonance frequency (f_o) is about 135 MHz. The phase velocity of the excited SAW can be derived to be ~4590 m/s by applying the relation of $v = f_o\lambda$. The SAW properties were evaluated by measuring the transfer function S_{21} in the SAW delay line using an Agilent 8753ES network analyzer. The typical transfer function S_{21} of the fabricated SAW devices exhibits an insertion loss of ~30.7 dB. The large reduction in out-of-band rejection is due to electromagnetic coupling between the input and output IDTs through the conductive Si substrate.[16,17] The change in resonance frequency due to the adsorption of nanoparticle conjugates can be used as the sensor response.

The silanized SAW devices were first immersed in a solution of 12.8 nM probe DNA-Au nanoparticle conjugates
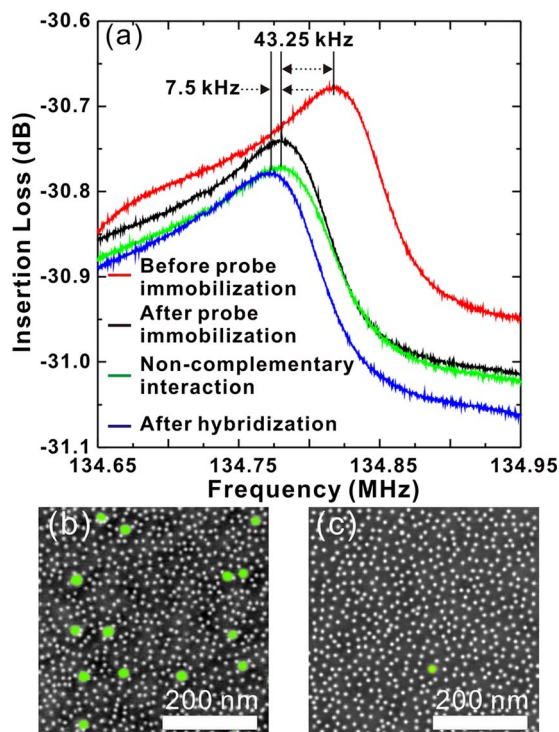
FIG. 4. (Color online) (a) Shifts in the resonant peak at 134.823 MHz after different surface treatments. (b) False-color FE-SEM micrograph after the step of DNA hybridization. (c) False-color FE-SEM micrograph after non-complementary interaction.

for 2 h, and then rinsed with water, and blow dried with nitrogen. In this step, probe oligonucleotides were bound onto the AlN surface via 10 nm Au nanoparticles to form the sensing layer for DNA detection. In the second step, DNA hybridization was performed with target DNA-Au nanoparticle conjugates (1.6 nM). The transfer function S_{21} was recorded before and after each step, and the corresponding shifts in resonant frequency were obtained [Fig. 4(a)]. The observed frequency shift due to probe oligonucleotides bound onto the APTMS-AlN surface after 2 h contact with 10 nm Au nanoparticles is $\sim 43.25 \pm 0.25$ kHz. Also, the frequency shift after DNA hybridization for 30 min is $\sim 7.5 \pm 0.25$ kHz. As shown in Fig. 4(a), the frequency shift after noncomplementary interaction is almost not detectable. The corresponding FE-SEM micrographs after DNA hybridization and noncomplementary interaction are shown in Figs. 4(b) and 4(c), respectively. The surface densities of target DNA-Au nanoparticle conjugates due to specific (DNA hybridization) and noncomplementary adsorption of 20 nm Au nanoparticles were found to be 55 ± 7 and 5 ± 4 μm^{-2}, respectively. The occurrence of noncomplementary adsorption ($\sim 10\%$) is likely caused by residue electrostatic adsorption since the solution conditions have been changed and the APTMS monolayer is no longer completely "neutralized" by 10 nm Au nanoparticles.

In our previous study, we estimated that the amounts of oligonucleotides bound to the surfaces of 10 and 20 nm Au nanoparticles are about 60 and 240, respectively.[10] Based on the Au mass density and the molecular weight of used oligonucleotides, the masses of DNA-Au nanoparticle conjugates can be estimated to be ~ 10.9 and ~ 83.6 ag, respectively. Thus, the SEM-measured surface mass densities of probe and target DNA-Au nanoparticle conjugates are ~ 2980 and ~ 460 ng/cm^2, respectively. In comparison, the observed SAW frequency shifts ($\sim 6:1$) are in reasonable agreement with the SEM-measured mass loadings. Moreover, the SAW mass sensitivity using the present AlN devices can be determined to be ~ 15 Hz cm^2/ng, about two orders of magnitude larger than that of the conventional quartz crystal microbalance sensors.[10]

In summary, we have demonstrated a generic surface biofunctionalization scheme for PA-MBE-grown AlN epitaxial films using organosilane molecules terminated with protonated amine groups and DNA-Au nanoparticle conjugates. The results shown here confirm the feasibility of Au-nanoparticle-enhanced SAW biosensors using AlN epitaxial films as both piezoelectric transducers and sensing media. This scheme is applicable for other biological molecules such as proteins, enzymes, and antibodies. These hybrid organ/inorganic interfaces can provide unique opportunities in diverse biosensor fields.

[1] M. Stutzmann, J. A. Garrido, M. Eickhoff, and M. S. Brandt, Phys. Status Solidi A **203**, 3424 (2006).
[2] N. Chaniotakis and N. Sofikiti, Anal. Chim. Acta **615**, 1 (2008).
[3] B. Baur, G. Steinhoff, J. Hernando, O. Purrucker, M. Tanaka, B. Nickel, M. Stutzmann, and M. Eickhoff, Appl. Phys. Lett. **87**, 263901 (2005).
[4] C.-F. Chen, C.-L. Wu, and S. Gwo, Appl. Phys. Lett. **89**, 252109 (2006).
[5] J. R. M. Petoral, Jr., G. R. Yazdi, A. L. Spetz, R. Yakimova, and K. Uvdal, Appl. Phys. Lett. **90**, 223904 (2007).
[6] G. Steinhoff, O. Purrucker, M. Tanaka, M. Stutzmann, and M. Eickhoff, Adv. Funct. Mater. **13**, 841 (2003).
[7] B. S. Kang, F. Ren, L. Wang, C. Lofton, W. W. Tan, S. J. Pearton, A. Dabiran, A. Osinsky, and P. P. Chow, Appl. Phys. Lett. **87**, 023508 (2005).
[8] B. S. Kang, S. J. Pearton, J. J. Chen, F. Ren, J. W. Johnson, R. J. Therrien, P. Rajagopal, J. C. Roberts, E. L. Piner, and K. J. Linthicum, Appl. Phys. Lett. **89**, 122102 (2006).
[9] B. Baur, J. Howgate, H.-G. von Ribbeck, Y. Gawlina, V. Bandalo, G. Steinhoff, M. Stutzmann, and M. Eickhoff, Appl. Phys. Lett. **89**, 183901 (2006).
[10] C. S. Chiu and S. Gwo, Anal. Chem. **80**, 3318 (2008).
[11] Y. Takagaki, P. V. Santos, E. Wiebicke, O. Brandt, H.-P. Schönherr, and K. H. Ploog, Appl. Phys. Lett. **81**, 2538 (2002).
[12] C. Caliendo and P. Imperatori, Appl. Phys. Lett. **83**, 1641 (2003).
[13] J. Xu, J. S. Thakur, F. Zhong, H. Ying, and G. W. Auner, J. Appl. Phys. **96**, 212 (2004).
[14] C.-L. Wu, J.-C. Wang, M.-H. Chan, T. T. Chen, and S. Gwo, Appl. Phys. Lett. **83**, 4530 (2003).
[15] C. A. Mirkin, R. L. Letsinger, R. C. Mucic, and J. J. Storhoff, Nature (London) **382**, 607 (1996).
[16] M. Clement, L. Vergara, J. Sangrador, E. Iborra, and A. Sanz-Hervás, Ultrasonics **42**, 403 (2004).
[17] I. Ingrosso, S. Petroni, D. Altamura, M. De Vittorio, C. Combi, and A. Passaseo, Microelectron. Eng. **84**, 1320 (2007).